ISIJ International, Vol. 58 (2018), No. 2, pp. 333–339

Austenite Grain Growth Kinetics after Isothermal Deformation in Microalloyed Steels with Varying Nb Concentrations

Kofi Ahomkah ANNAN,* Charles Witness SIYASIYA and Waldo Edmund STUMPF

Department of Materials Science and Metallurgical Engineering, University of Pretoria, 0002, Pretoria, South Africa.

(*Received on August 15, 2017; accepted on October 10, 2017*)

Grain growth equation constants n, Q and A for Nb bearing steels with the Nb varying from 0.002 wt% to 0.1 wt%, were experimentally determined under reheating and high temperature hot rolling roughing conditions. The constants from these treatments were then used to develop constitutive equations that incorporate the initial grain size D_o and a Nb-effect for grain growth predictions in these steels. Comparative analysis of the results showed that the values of the constants generated under rough rolling deformation conditions were slightly higher than those generated under reheating conditions. The activation energy for grain boundary migration Q was found to be in the range of 256 to 572 kJ/mol, the exponential constant n ranged from 2.6 to 6.5 and the material and processing condition's constant A was found to range from 5.23×10^{11} to 4.96×10^{28} in all cases as a function of the Nb content. Analysis of the influence of the initial grain size D_o showed that any contribution of D_o can be neglected unless it is equal or more than 70 percent of the average size of the measured austenite grain size D. A logical degree of precision in predicting austenite grain growth in microalloyed steels with different Nb contents, has been achieved in the current work.

KEY WORDS: grain growth; microalloyed; deformation; reheating.

1. Introduction

Grain growth in microalloyed steels has been studied extensively in the last two decades with some equations developed to predict the growth behaviour in these steels.[1–3] The addition of microalloying elements (Nb, Ti, or V) results in precipitation of finely dispersed precipitates, which may retard austenite grain growth through grain boundary pinning.[4,5] The associated evolution of particle size and volume fraction produces a change in the pinning force that controls the austenite grain growth through Zener pinning and the microstructural changes.[5–7] In steels, austenite grain size is a microstructural parameter that must be carefully controlled during heat treatment.[4,6–8] With conventional approaches (*e.g.* Metallography), the on-line *in situ* monitoring of austenite grain growth at high temperatures is not feasible. Alternative on-line technique is the laser ultrasonic, which is costly due to the special equipment, required.[9] Predicting the austenite grain growth behaviour based on processing conditions is the ideal option. Several attempts have been made to empirically develop equations to predict the austenite grain growth behaviour in steels bearing microalloying elements (MAE).[1–4,10–12] The setting of n to a constant value makes it easier to plot lnD^n as a function of the inverse temperature (1/T) in order to obtain Q.[1–3,13,14] The constant n is dependent on the alloy composition as well as the processing conditions.[1–4] It has been pointed out that, under changing processing conditions, the value of n is expected to correlate with the processing conditions (temperature).[2] Thus, the use of a fixed value of n for prediction of grain growth under changing processing conditions and varying compositions will lead to deviation in the prediction, as the value of n cannot in this sense correlate with the temperature or the composition.

The comparison of the grain growth constants n, Q and A generated under reheating and deformation conditions as well as the effect of these conditions on the parameters with changing D_o value has not been considered to date and this has been adequately addressed in this current work.

2. Experimental Material and Procedure

Table 1 shows the chemical composition of the steels used in the study. In this study, reheating tests were employed to investigate the effect of soaking temperature

Table 1. Chemical composition of the steels used in the study.

Steel	Chemical composition (mass%)								
	C	Mn	Si	Nb	Ti	V	Al	N	Ni
0.002 Nb	0.17	1.13	0.11	0.002	0.001	0.007	0.05	0.018	0.15
0.03 Nb	0.16	1.15	0.15	0.03	0.02	0.008	0.02	0.018	0.15
0.05 Nb	0.17	1.15	0.15	0.05	0.02	0.009	0.03	0.019	0.15
0.07 Nb	0.14	1.10	0.15	0.07	0.02	0.006	0.04	0.020	0.17
0.10 Nb	0.18	1.27	0.15	0.10	0.02	0.009	0.04	0.020	0.17

* Corresponding author: E-mail: kofi.annan@up.ac.za
DOI: http://dx.doi.org/10.2355/isijinternational.ISIJINT-2017-464

© 2018 ISIJ

and deformation on the influence of deformation temperature on grain growth. The samples (5 mm diameter × 10 mm length) were homogenized at 1 150°C for 5 minutes to ensure elimination of thermal gradients before taken to the austenitization temperature (1 100, 1 150, 1 200, 1 220, or 1 250°C) at a rate of 4°C.min^{-1} and held there for predetermined austenitizing times (0, 10, 30, 60 90, or 120 minutes). **Figure 1** shows a schematic profile of the heat treatment schedule followed in this test.

The samples were taken to the deformation temperature (1 000, 1 050, 1 100 and 1 150°C) at 5°C s^{-1} after homogenization where it was held at the test temperature for 20 s where after a single hit compression was applied to a strain of 0.4 and at a strain rate of 0.1 s^{-1} in the Bähr™ deformation-dilatometer under an argon atmosphere. The samples were then held after compression at the deformation temperature for respective times of 0, 10, 30, 60, 90 or 120 minutes before cooling at a rate of 600°C/s to room temperature. The scheduled profile followed in the single hit compression test is shown in **Fig. 2**.

Both the reheated and deformed samples were tempered at 490°C for 72 hours to improve the response of prior austenite grain boundaries to etching. The samples were etched in a picric acid solution containing 100 ml saturated aqueous picric acid, 100 ml distilled water, 4 g sodium tridecylbenze sulfonate and 2–3 drops of triton. The grain size was measured using a quantitative metallographic technique (linear intercept method) according to ASTM E112, ensuring that at least 300 grain intersections were counted for each of the samples. In this study, the grain size of the samples held for zero (0) minutes after soaking for 5 minutes at 1 150°C were used as the initial grain size D_o of the austenite grain size at that temperature.

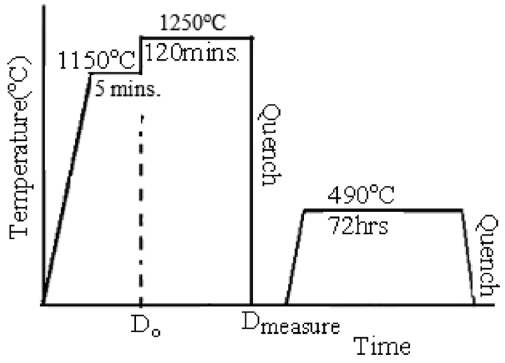

Fig. 1. Schematic illustration of thermal cycle for the isothermal heat treatment.

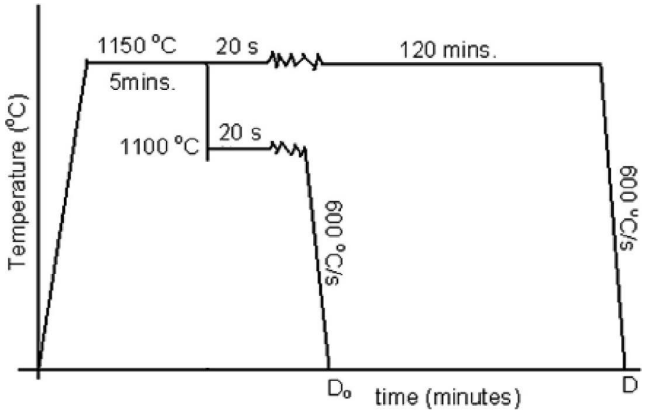

Fig. 2. Schematic representation of the deformation process on the Bähr dilatometer.

3. Results

3.1. The Solubility Behavior of the Precipitates

The volume fractions of precipitates as a function of the temperature predicted by Thermocalc for the steels used in the study, are shown in **Fig. 3**. These show that the testing temperature range of 800–1 250°C will lead to dissolution of quite a substantial amount of the precipitates but not to a complete dissolution of all particles. The presence of precipitates in the steels at the TMCP conditions considered in this study means that a unimodal grain size structure can be expected if these precipitates are effective in pinning the grain boundaries.[5,14,15)]

3.2. Microstructure and Grain Size Distribution

Optical micrographs revealing the prior austenite grain morphologies as well as histograms showing the grain size distributions in the reheat and deformed Nb steels are shown in **Fig. 4**.

The difference in grain sizes observed under the two conditions in the steels is due to the temperatures employed during the two processes. The deformation temperature range (1 000°C–1 150°C) is lower than the reheating temperatures (1 100–1 250°C) employed. The volume fraction of precipitates present in the steels at the deformation temperature is higher than at the reheating conditions hence higher grain growth control is observed in the deformation process leading to smaller starting grain sizes $D_{0.}$. The Zener pinning forces offered by the precipitates in these steels are also found to be more effective than the driving force for grain growth, hence greater grain growth inhibition.[5,6,15,16)]

3.3. Transmission Electron Microscopy

Figure 5 shows the STEM images of precipitates observed by TEM after reheating of 0.03%Nb steel at different austenitizing temperatures.

The round-shaped precipitates shown in Fig. 5(a) were confirmed by STEM EDX analysis to be NbC with a size less than 40 nm whiles the rectangular-shaped particles in Figs. 5(b) and 5(c) were confirmed to be TiC with sizes less than 30 nm. It is noted that the Nb precipitates continually dissolved into the matrix during the reheating process as exhibited in Figs. 5(a)–5(c).[5,7,17)] It was observed that the atomic ratio of Nb to Ti contained within these precipitates continually reduced with the increase in austenizing temperature. The composition of Nb to Ti in the precipitates changed from near equal at 1 000°C to Ti-rich (Ti, Nb) C and (Ti, Nb) N at 1 200°C.

3.4. Effect of Increased Nb Content on the Austenite Grain Growth in the Steels

The quantitative analysis of the optical measurement of austenite grain size (AGS) shown in **Fig. 6** confirms the substantial influence of the increased Nb content as well as processing condition on austenite grain growth inhibition in the steels. It is evident from this figure, that the steel con-

© 2018 ISIJ

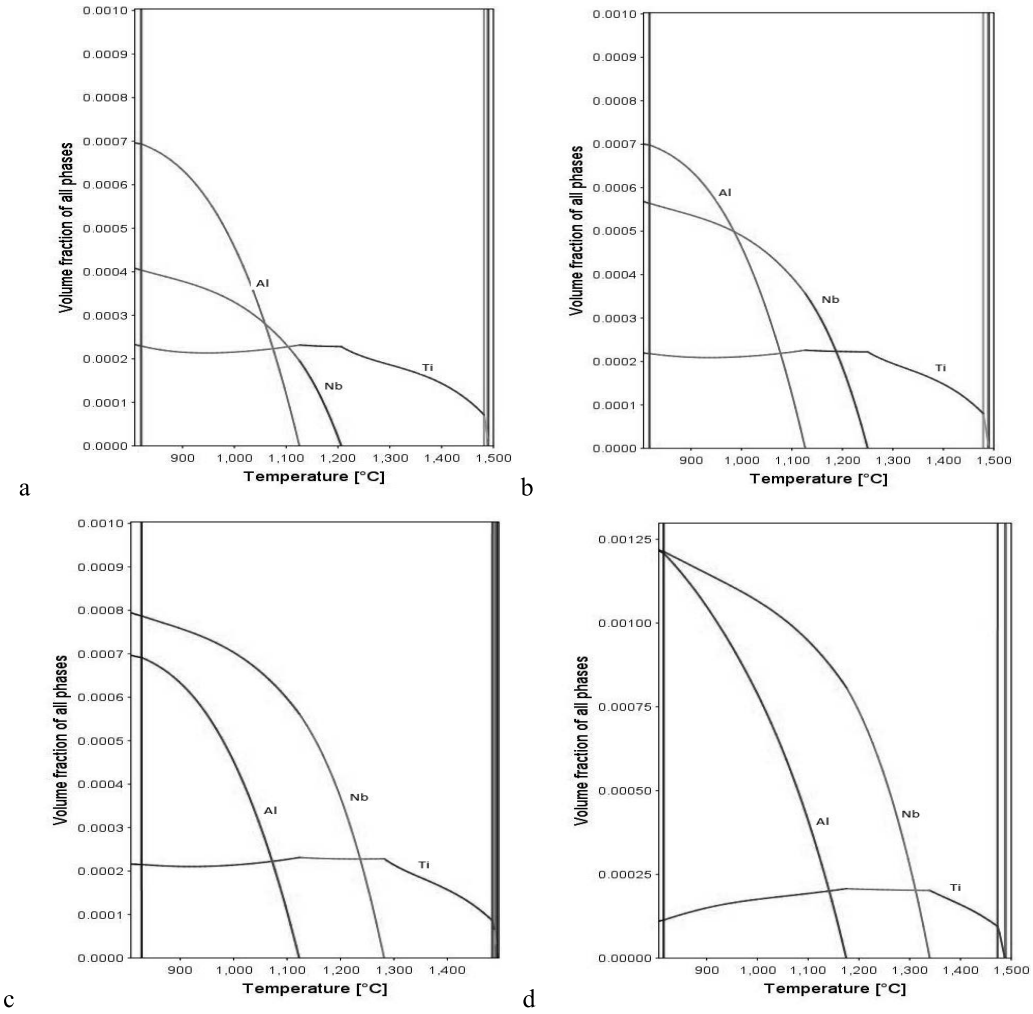

Fig. 3. Thermocalc predictions of the volume fraction of precipitates in the Nb-bearing steels with (a) 0.03%Nb (b) 0.05% Nb (c) 0.07% Nb and (d) 0.1% Nb.

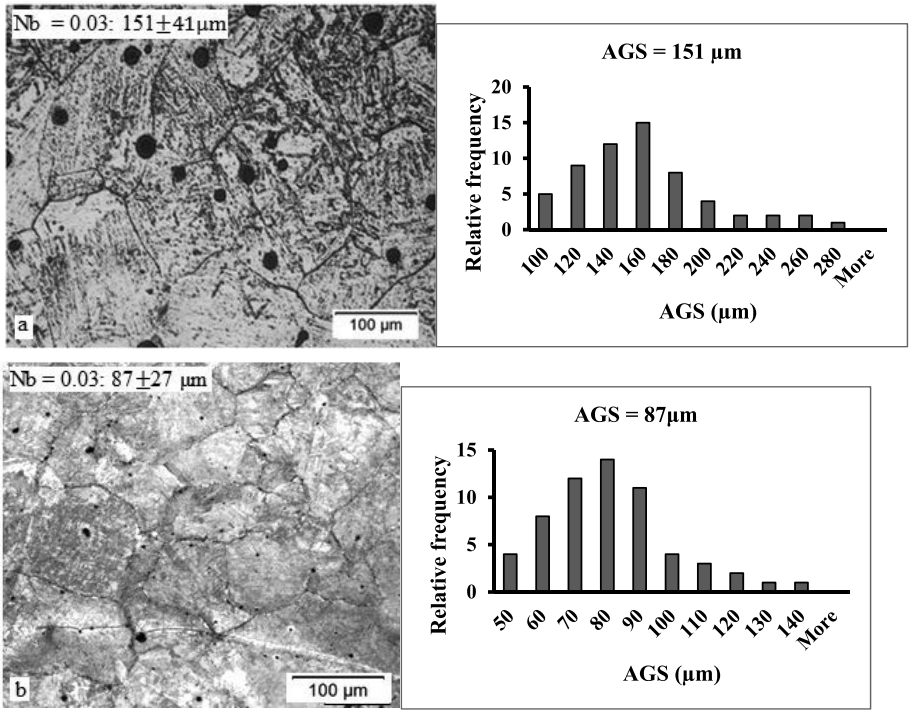

Fig. 4. Optical micrographs and grain size distribution plots of prior austenite in (a) 0.03% Nb steel heat treated at an austenitizing temperature of 1 250°C and for holding times of 120 minutes (b) 0.03% Nb steel soaked for 5 minutes at 1 150°C, deformed at 1 150°C at a strain rate of 0.1 s^{-1} and to a strain of 0.4 and held for 120 minutes at 1 150°C.

© 2018 ISIJ

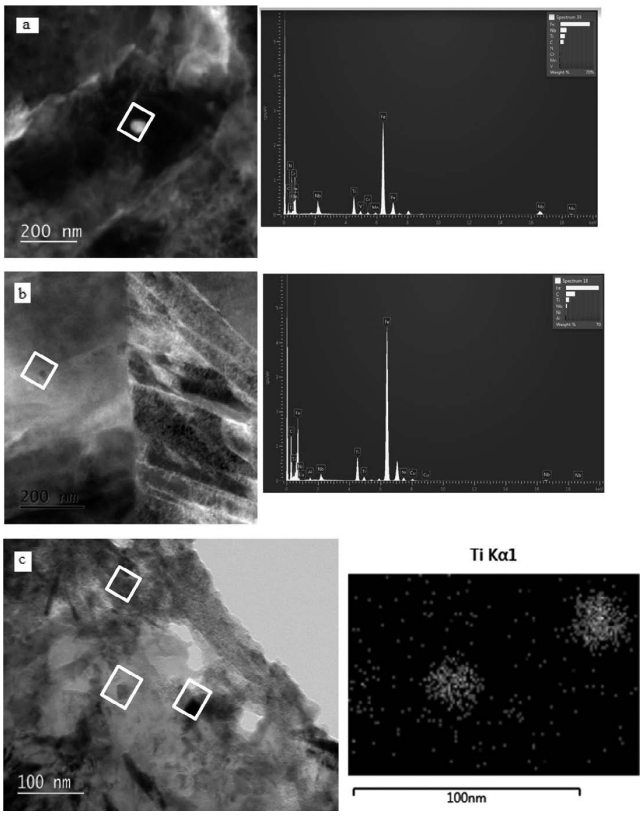

Fig. 5. HAADF STEM micrographs and STEM EDX for 0.03 mass% Nb steel austenitized at a). 1 000°C, b). 1 100°C and c). 1 200°C.

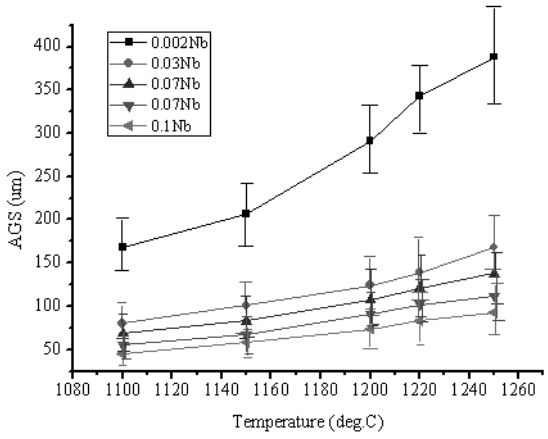

a.

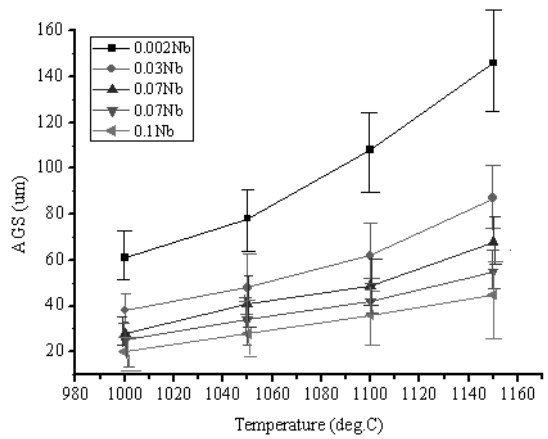

b.

Fig. 6. Influence of Nb content on austenite grain growth inhibition in Nb containing steels during (a) reheating (b) reheating followed by deformation and holding for 120 minutes.

taining 0.1% Nb prevented austenite grain growth the most as it produced the smallest grain sizes whilst the 0.002% Nb steel prevented the austenite grain growth the least by producing larger grain sizes. The Thermocalc™ predictions of volume fractions of Nb precipitate in the studied steels was found to be in increasing order of 0.002% Nb < 0.03%, Nb <0.05%, Nb <0.07%, Nb <0.1% Nb.

In comparison of the reheat conditioned steel with that of the deformed steels, the latter produced smaller grain sizes owing to a high presence of precipitates and the dynamically recrystallized nature of the deformed samples as exhibited in the curves shown in **Fig. 7**.[8,18–20]

3.5. Determination of the Austenite Grain Growth Constants *n*, *Q* and *A*

The Sellars and Whiteman[18] classical equation shown in Eq. (1), was employed in determining the grain growth constants

$$D^n - D_o^n = A\, exp\left(-\frac{Q}{RT}\right)t \quad \ldots\ldots\ldots\ldots\ldots (1)$$

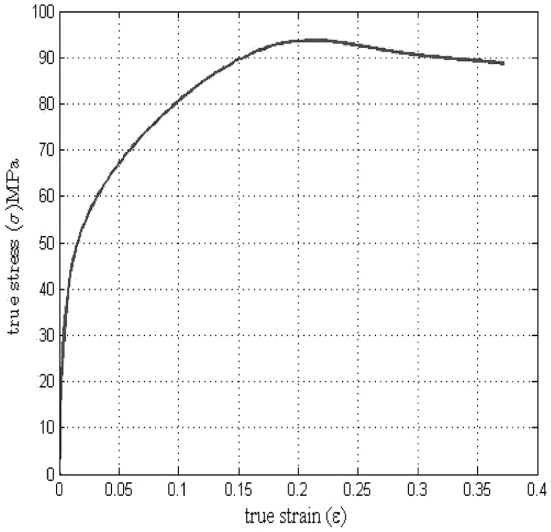

Fig. 7. True stress–strain curves for 0.03%Nb steel deformed at a strain rate of 0.1 s^{-1}, strain of 0.4 and temperature of 1 100°C.

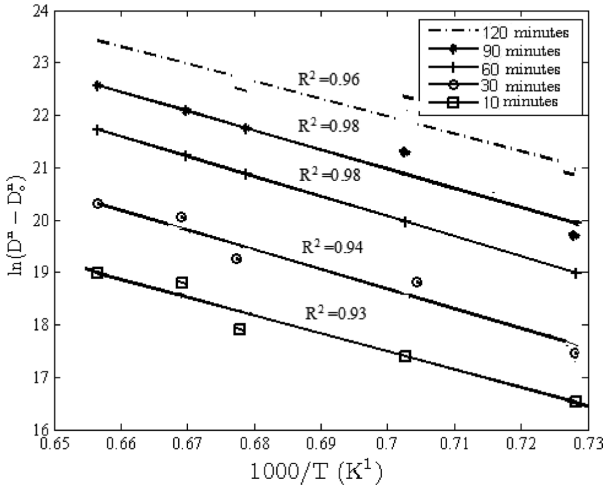

Fig. 8. Matlab plot of the natural log of the average grain size as a function of the inverse of the absolute temperature for the 0.03 Nb steel.

© 2018 ISIJ

where T is the absolute temperature, t is the time, Q is the activation energy for grain boundary migration, A is a constsnt encompassing material and processing conditions and R is the universal gas constant. Iterative tests of straight line regression coefficients R^2 of experimentally measured austenite grain sizes using Eq. (1), were used to determine the exponent n.[21] In this analysis, the plot of the second differential of R^2, $(dR^2)^2/dn^2$ as a function of n gave a maximum correlation value of n at $(dR^2)^2/dn^2 = 0$. The plot of solution to Eq. (1), which is comparable to the equation of a straight line, is shown in **Fig. 8**. Comparative analysis of the linear solution to Eq. (1) with the equation of a straight line made it possible for the constants Q and A to be determined. Thus; $-Q = R \times$ slope (while the slope is negative) and $A = e^C/t$ where, c is the intercept and t is the austenitizing time.

A comparative analysis of the differences in constants generated under reheating (HT) and deformation (DF) conditions for the steels are presented in **Table 2**.

In these steels, slightly higher values were recorded in constants generated under deformation conditions as compared to the reheating conditions. These higher values could be attributed to the comparable smaller grain sizes obtained in the deformation process due to higher volume fraction of precipitates present in the steel during the lower deformation temperatures as predicted by Thermocalc™. The higher differences in constants between the two processes were recorded in the constants Q followed by A and n.

3.6. Development of the Constitutive Equations

The obtained data from optically measured grain sizes were analyzed to obtain the grain growth equation's constants n, Q and A as in section 3.5, were quantitatively expressed as a function of the Nb content as shown in the plots in **Fig. 9**.

The analysis of the plots shown in Fig. 9, made it possible for constitutive equations to be developed using the coefficients generated as in Eqs. (2) and (3) for reheating and deformation (with the subscripts RH and DF referring to Reheating and Deformation respectively).

$$D_{RH} = \left[D_o^{n_{RH}} + \left(A_{RH} e^{-\frac{Q_{RH}}{RT}} \right) t \right]^{1/n_{RH}} \quad \text{..... (2)}$$

$$D_{DF} = \left[D_o^{n_{DF}} + \left(A_{DF} e^{-\frac{Q_{DF}}{RT}} \right) t \right]^{1/n_{DF}} \quad \text{..... (3)}$$

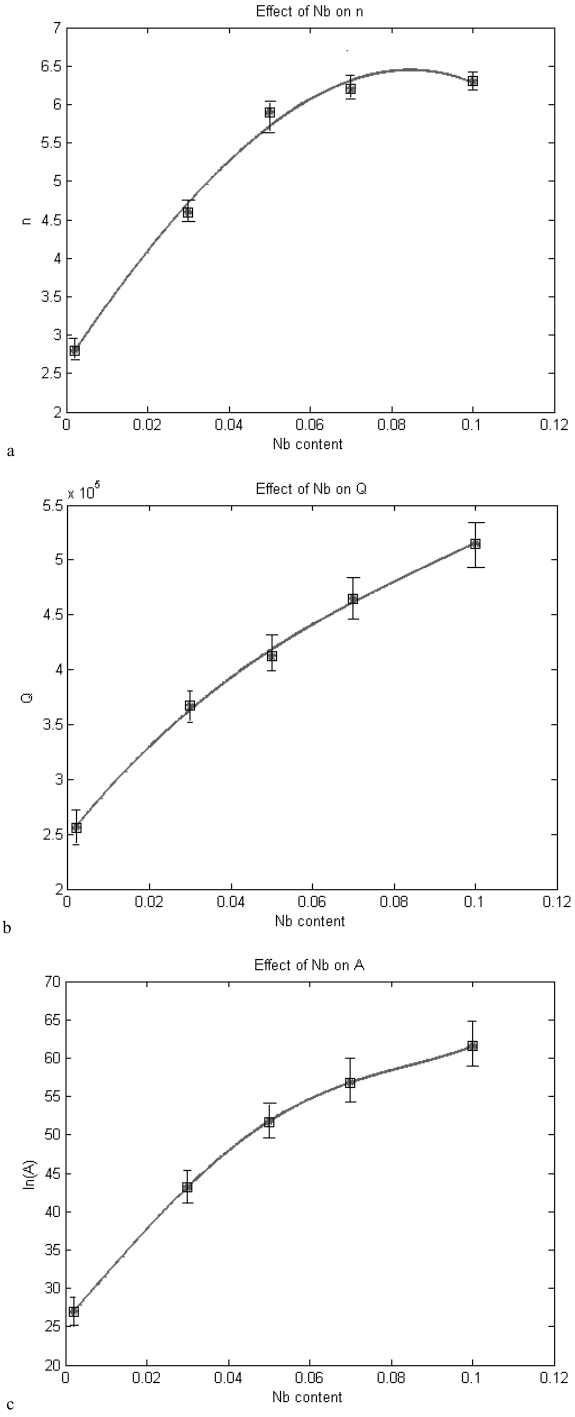

Fig. 9. The effect of Nb content (in mass%) in the steels on the experimentally determined (a) grain growth exponent n, (b) activation energy Q in KJ/mol and (c) material and processing constant A.

Table 2. Differences between the generated constants' values from reheating and deformation data.

Constants generated for microalloyed steels									
Alloy	n		Q (kJ/mol)		A		Differences between HT and DF values		
	HT	DF	HT	DF	HT	DF	Δn	ΔQ	ΔA
0.002 mass% Nb	2.6	2.8	256	276	5.22E+11	4.24E+12	0.2	20	3.72E+12
0.03 mass% Nb	4.5	4.6	367	417	5.46E+18	1.33E+22	0.1	50	1.33E+22
0.05 mass% Nb	5.7	5.9	412	467	2.91E+22	7.94E+23	0.2	55	7.65E+23
0.07 mass% Nb	6.0	6.2	465	521	4.69E+24	9.63E+24	0.2	56	4.94E+24
0.1 mass% Nb	6.2	6.5	515	572	5.46E+26	4.96E+28	0.3	57	4.91E+28

HT = Heat treatment DF = Deformation

© 2018 ISIJ

Table 3. Effect of the D_o value on the prediction of D in 0.07 mass%Nb steel reheated at 1 250°C and held for 120 minutes.

	D	D_o	40%D	50%D	60%D	70%D	80%D	90%
D_0 value in μm as a % of D	101	38	40	50	61	71	81	91
Predicted value in μm of D	101	101	101	101	103	105	108	112

where n_{RH}, n_{DF}, A_{RH}, A_{DF}, Q_{RH} and Q_{DF} which are expressed as a function of the %Nb content are as shown in Eqs. (4)–(9), below:

$$n_{RH} = -67\,537\mathrm{Nb}^3 + 2\,527.5\mathrm{Nb}^2 + 73.787Nb + 3.7069 \quad \ldots (4)$$

$$n_{DF} = -1\,615.4\mathrm{Nb}^2 + 123.27\mathrm{Nb} + 4.0413 \quad \ldots\ldots (5)$$

$$Q_{RH} = 3\times10^6 Nb + 320\,216 \quad \ldots\ldots (6)$$

$$Q_{DF} = 3\times10^6 Nb + 373\,004 \quad \ldots\ldots (7)$$

$$A_{RH} = \exp\{408.5\mathrm{Nb} + 39.404\} \quad \ldots\ldots (8)$$

$$A_{DF} = \exp\{391.12\mathrm{Nb} + 44.961\} \quad \ldots\ldots (9)$$

3.7. Influence of the Initial Grain Size D_o on the Grain Growth Prediction in Microalloyed Steels

Table 3 show the analysis of influence of D_o on the prediction of austenite grain growth in the microalloyed steels. The effect of the initial grain size D_o on the prediction of the final grain size D in the constitutive equation was evaluated using increasing percentages of the starting grain size D_o with respect to the final measured grain size D in predicting D. It was observed that the value used for D_o influences the prediction of the final grain size D only measurably when it is about 70% or larger than that of the final grain size D.

4. Discussion

4.1. Austenite Grain Growth Inhibition in the Microalloyed Steels

Figure 4 indicates that the austenite grain growth inhibition decreases with an increase in temperature owing to depletion of precipitates with increasing temperature as shown in Fig. 5. It is further shown that the austenite grain growth rate during processing is dependent on the composition, the heating temperature and the holding time as shown in Fig. 6.[5,8,11,20] The grain growth rate decreased with an increase in Nb content as shown by the Thermocalc™ predictions in Fig. 3. The equilibrium dissolution rate of Nb and C decreased considerably with increasing temperature. Whereas Nb and C dissolves at or beyond 1 200°C the reheating temperature used in the current investigation went up to 1 250°C, hence the considerable decrease in the pinning effect in the reheated steels as measured against the deformed steels which were carried out within the range of 1 000°C to 1 150°C. However, with deformation carried out below the dissolution temperature of Nb and Ti nitride and carbide precipitates led to the increase in the presence of the more stable TiNb carbonitrides which produced much higher pinning forces, thereby suppressing the grain growth in the steels during deformation and lowering the coarsening rate during deformation more than during reheating.[1,2,5]

Pinning particles' effectiveness has been reported to depend on their size and distribution as well as the particle's ability to resist coarsening at especially higher temperatures.[5,15–18] From Zener's basic pinning equation, $p = (3\gamma Vv)/2r$, it can be seen that either an increase in volume fraction V_v or a decrease in particle size r of precipitates will lead to an increase in the pinning force, which eventually causes a decrease in the grain size.[18] This therefore, explains that grain growth inhibition can be achieved through a processing condition that will either lead to a higher volume fraction of precipitates or a smaller particle size.[6] From the Thermocalc predictions, it shows that at sufficiently higher temperatures, as seen under the reheating condition in the current work, the volume fraction of precipitates begins to decrease owing to dissolution of particles. This, therefore, indicates that the ability of the precipitates to pin austenite grain boundaries effectively decreases with increasing temperature as was shown by the Thermocalc™ predictions and the TEM images in Figs. 3 and 5 respectively. The solidification rate as well as the temperature at which the particles precipitate determines the particles' size and particle distribution in the microalloyed steels.[5,20] This evidently explains why the smaller particle sizes and higher volume fractions of precipitates is predicted and is observed in the samples deformed, more so than those in the reheated condition only. This accounts for the smaller grain sizes recorded under the deformation conditions than in the reheating conditions.

4.2. The Influence of Nb Content on the Constants n, Q and A

An increase in Nb content leads to an increase in the volume fraction of Nb precipitates. For instance, the volume fraction of Nb precipitates in 0.03%Nb steel at 1 100°C was calculated by Thermocalc™ at 0.35% whilst the value in the 0.07%Nb alloy at the same temperature was found to be 0.55%. The particle size of the Nb precipitate was also found to decrease with an increase in the Nb content.[21] This was determined by TEM analyses but also arises from the higher Gibbs driving force for nucleation and hene a higher nucleation art in the higher Nb-content alloy. The increase in volume fraction and decrease in particle size greatly increases the pinning force of the grain boundary according to Zener's pinning equation $p = 3\gamma Vv/2r$. The volume fraction of precipitates was also calculated by Thermocalc™ to decrease with increasing temperature whilst the particles size increases with increasing temperature due to coarsening. The increase in the volume fraction and decrease in particle size with an increase in Nb content as well as lower temperatures produced higher pinning forces leading to smaller grain sizes and subsequently higher values for n, Q and A under deformation conditions. The pinning forces decreased significantly with a decrease in Nb content and also at higher temperatures due to the lesser volume frac-

© 2018 ISIJ

tion of precipitates and larger particle size. This decreased the boundary pinning force, which led to larger grain sizes and eventually smaller values of the grain growth constant generated under reheating conditions as opposed to deformation conditions.

4.3. Predictive Potential of the Current Study's Constitutive Equations

The analysis of the results show that in both the deformed and the reheated conditions the predictions made by the current study are very close to the measured values within a temperature range of 1 000°C–1 150°C. The predictions made in the Nb-bearing steels slightly *over-estimated* at lower temperatures (<1 150°C) and *under-estimated* at higher temperatures (>1 150°C).[1–3] These observed differences in the predictions may be attributed to the effect of other microalloying and alloying elements, which are not accounted for by the equations. Despite these differences, a reasonably acceptable degree of prediction was achieved with the developed constitutive equations. **Figures 10**(a) and 10(b) show a reasonable agreement between measured and predicted grain sizes from the developed constitutive equations for the reheating and the deformed conditions respectively.

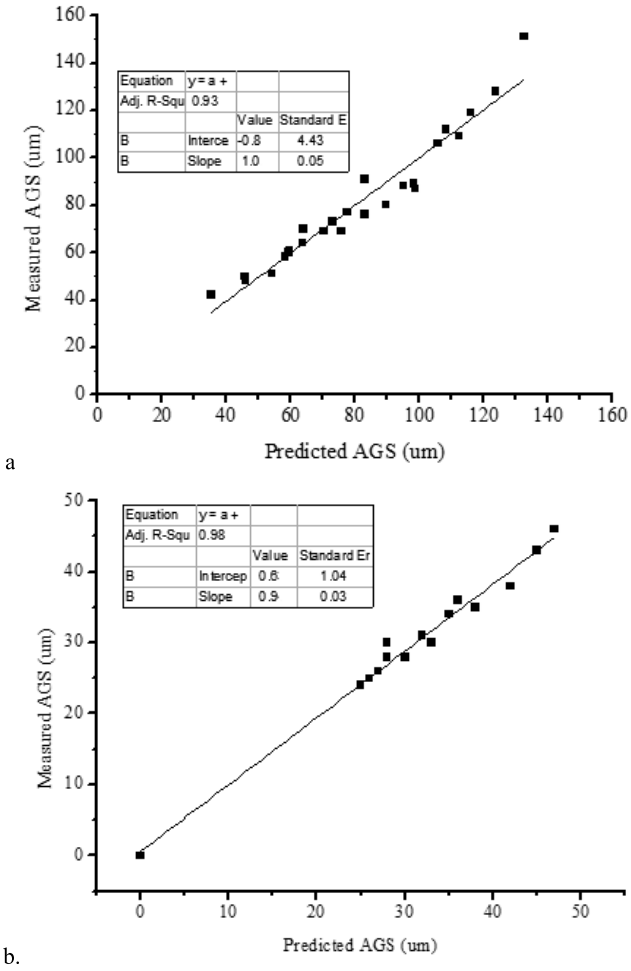

Fig. 10. Reliability of the isothermal constitutive grain growth equation through comparison of measured and predicted grain sizes for (a) 0.03% Nb steel during reheating (b) 0.07% Nb steel during deformation (Note that in both cases the fitted line was "forced" through zero).

5. Conclusion

- Constitutive grain growth equation constants n, Q and A determined for the studied microalloyed steels were found to be higher under deformation conditions than reheating conditions.
- The constants n, Q and A found under deformation conditions were 2.8 to 6.5, 276 to 572 kJ/mol, and 4.24×10^{12} to 4.96×10^{28} respectively whereas constants n, Q and A found under reheating conditions were 2.6 to 6.2, 256 to 515 kJ/mol, and 5.22×10^{11} to 546×10^{26} respectively
- The initial grain size D_o was found to be effective in influencing the grain size prediction only if it is about seventy percent (70%) or greater of the actual austenite grain size D.

Acknowledgements

Permission from the University of Pretoria to publish this work is duly acknowledged.

Funding: The National Research Foundation (NRF) of the Republic of South Africa supported this work.

REFERENCES

1) P. D. Hodgson and R. K. Gibbs: *ISIJ Int.*, **32** (1992), 1329.
2) H. R. Wang and W. Wang: *Mater. Sci. Technol.*, **24** (2008), 228.
3) S. Nanba, M. Kitamura, M. Shimada, M. Katsumata, T. Inoue, H. Imamura, Y. Maeda and S. Hattori: *ISIJ Int.*, **32** (1992), 377.
4) P. A. Manohar, D. P. Dunne, T. Chandra and C. R. Killmore: *ISIJ Int.*, **36** (1996), 194.
5) P. Gong, E. J. Palmiere and W. M. Rainforth: *Acta Mater.*, **7** (2015), 392.
6) C. Zener, quoted by C. Smith: *Trans. AIME*, **175** (1948), 47.
7) L. Gavard, F. Montheillet and L. J. Coze: *Scr. Metall. Mater.*, **39** (1998), 1095.
8) K. Matsuura and Y. Itoh: *ISIJ Int.*, **31** (1991), 366.
9) M. Maalekian, R. Radis, M. Militzer, A. Moreau and W. J. Poole: *Acta Mater.*, **60** (2012), 1015.
10) D. Bhattacharya: *Technol. Metall. Mater. Min.*, **11** (2014), No. 4, 371.
11) S. Jiao, J. Penning, F. Leysen, Y. Houbaert and E. Aernoudt: *ISIJ Int.*, **40** (2000), 1035.
12) S. Du, Y. Li and Y. Zheng: *J. Mater. Eng. Perform.*, **25** (2016), 2661.
13) S. Lee and Y. Lee: *Mater. Des.*, **29** (2008), 1840.
14) S. Uhm, J. Moon, C. Lee, J. Yoon and B. Lee: *ISIJ Int.*, **44** (2004), 1230.
15) K. Xu and B. G. Thomas: *Metall. Mater. Trans. A*, **43** (2012), 1079.
16) N. Isasti, D. Jorge-badiola, M. L. Taheri and P. Uranga: *Metall. Mater. Trans. A*, **44A** (2013), 3552.
17) B. Ma, Y. Peng, B. Jia and Y. Liu: *J. Iron Steel Res. Int.*, **17** (2010), 61.
18) C. M. Sellars and J. A. Whiteman: *Met. Sci.*, **13** (1979), 187.
19) Q. B. Yu and Y. Sun: *Mater. Sci. Eng. A*, **420** (2006), 34.
20) S. C. Hong, S. H. Lim, H. S. Hong, K. J. Lee, D. H. Shin and K. S. Lee: *Mater. Sci. Technol.*, **20** (2004), 207.
21) K. A. Annan, C. W. Siyasiya, W. E. Stumpf, K. M. Banks and A. S. Tuling: *Adv. Mater. Res.*, **1019** (2014), 327.

© 2018 ISIJ